

Nonlinear Modeling, Estimation and Predictive Control in APMonitor

John D. Hedengren, Reza Asgharzadeh Shishavan

Department of Chemical Engineering, Brigham Young University, Provo, UT 84602

Kody M. Powell, Thomas F. Edgar

The University of Texas at Austin, Austin, TX, 78712

Abstract

This paper describes nonlinear methods in model building, dynamic data reconciliation, and dynamic optimization that are inspired by researchers and motivated by industrial applications. A new formulation of the ℓ_1 -norm objective with a dead-band for estimation and control is presented. The dead-band in the objective is desirable for noise rejection, minimizing unnecessary parameter adjustments and movement of manipulated variables. As a motivating example, a small and well-known nonlinear multivariable level control problem is detailed that has a number of common characteristics to larger controllers seen in practice. The methods are also demonstrated on larger problems to reveal algorithmic scaling with sparse methods. The implementation details reveal capabilities of employing nonlinear methods in dynamic applications with example code in both MATLAB and Python programming languages.

Keywords: advanced process control, differential algebraic equations, model predictive control, dynamic parameter estimation, data reconciliation, nonlinear control, dynamic optimization

1. Introduction

Applications of Model Predictive Control (MPC) are ubiquitous in a number of industries such as refining and petrochemicals [1]. Applications are also somewhat common in chemicals, food manufacture, mining, and other manufacturing industries [2]. Contributions by Morari and others have extended the MPC applications to building climate control [3, 4], stochastic systems [5, 6], induction motors [7], and other fast processes with explicit MPC [8, 9, 10, 11, 12, 13]. A majority of the applications employ linear models that are constructed from empirical model identification, however, some of these processes have either semi-

Email address: john.hedengren@byu.edu (John D. Hedengren)

10 batch characteristics or nonlinear behavior. To ensure that the linear models
11 are applicable over a wider range of operating conditions and disturbances, the
12 linear models are retrofitted with elements that approximate nonlinear control
13 characteristics. Some of the nonlinear process is captured by including gain
14 scheduling, switching between multiple models depending on operating condi-
15 tions, and other logical programming when certain events or conditions are
16 present. The art of using linear models to perform nonlinear control has been
17 refined by a number of control experts to extend linear MPC to a wider range of
18 applications. While this approach is beneficial in deploying applications, main-
19 tenance costs are increased and sustainability is decreased due to the complexity
20 of the heuristic rules and configuration.

21 A purpose of this article is to give implementation details on using nonlin-
22 ear models in the typical steps of dynamic optimization including (1) model
23 construction, (2) fitting parameters to data, (3) optimizing over a future pre-
24 dictive horizon, and (4) transforming differential equations into sets of algebraic
25 equations. Recent advancements in numerical techniques have permitted the di-
26 rect application of nonlinear models in control applications [14], however, many
27 nonlinear MPC applications require advanced training to build and sustain an
28 application. Perhaps the one remaining obstacle to further utilization of nonlin-
29 ear technology is the ease of deploying and sustaining applications by researchers
30 and practitioners. Up to this point, there remain relatively few actual industrial
31 applications of control based on nonlinear models. An objective of this paper
32 is to reduce the barriers to implementation of nonlinear advanced control ap-
33 plications. This is attempted by giving implementation details on the following
34 topics:

- 35 • nonlinear model development
- 36 • parameter estimation from dynamic data
- 37 • model predictive control with large-scale models
- 38 • direct transcription for solution of dynamic models

39 In addition to the theoretical underpinnings of the techniques, a practical
40 application with process data is used to demonstrate model identification and
41 control. The application used in this paper is a simple level control system
42 that was selected to illustrate the concepts without burdening the reader with
43 model complexity. In practice, much larger and more complex systems can be
44 solved using these techniques. An illustration of scale-up to larger problems
45 gives an indication of the size that can be solved with current computational
46 resources. The example problems are demonstrated with the APMonitor Op-
47 timization Suite [15] [16], freely available software for solution of linear pro-
48 gramming (LP), quadratic programming (QP), nonlinear programming (NLP),
49 and mixed-integer (MILP and MINLP) problems. Several other software plat-
50 forms can also solve dynamic optimization problems with a variety of modeling
51 systems, solution strategies, and solvers [17] [18] [19] [20] [21] [22].

52 Of particular interest for this overview is the transformation of the differ-
53 ential and algebraic equation (DAE) systems into equivalent NLP or MINLP
54 problems that can be solved by large-scale optimizers such as the active set
55 solver APOPT [23] and the interior point solver IPOPT [24]. Specific examples
56 are included in the appendices with commands to reproduce the examples in
57 this paper. Some other examples include applications of computational biology
58 [25], unmanned aerial systems [26], chemical process control [27], solid oxide fuel
59 cells [28, 29], industrial process fouling [30], boiler load following [31], energy
60 storage [32, 33, 34], subsea monitoring systems [35, 36, 37], and friction stir
61 welding of spent nuclear fuel [38].

62 This paper includes a number of innovative techniques for formulating large-
63 scale control and optimization problems. A dead-band is added to well-known
64 ℓ_1 -norm objective forms for estimation and optimization. This form is different
65 than the forms previously proposed [39] [40] in that it specifies a dead-band
66 for noise rejection and move suppression. The formulation allows for batch or
67 periodic control and avoids a separate steady-state target calculation. Similar
68 characteristics to prior work [41] include tuning for speed of response, ranked
69 utilization of manipulated variables (MVs), treatment of controlled variables
70 (CVs) with equal concern, and prioritization among separate sets of MVs and
71 CVs.

72 The objective form presented here for estimation and control is compared
73 to squared-error or ℓ_2 -norm objectives that are reported in the literature. The
74 appendices include concise source code that can be used to reproduce the results
75 or serve as a framework for further applications. The target audience is the
76 practitioner or researcher interested in applying nonlinear estimation and control
77 to nonlinear dynamic applications.

78 2. Nonlinear Modeling

79 A critical aspect of any controller is obtaining a sufficiently correct model
80 form. The model form may include adjustable parameters that are not di-
81 rectly measurable but can be tuned to match both steady-state and dynamic
82 data. Model identification involves adjustment of parameters to fit process data.
83 Models may be linear or nonlinear, empirical or based on fundamental forms
84 that results from material and energy balances, reaction kinetic mechanisms, or
85 other pre-defined model structure. The foundation of many of these correlations
86 is on equations of motion, individual reaction expressions, or balance equations
87 around a control volume such as $accumulation = inlet - outlet + generation -$
88 $consumption$. In the case of a mole balance, for example, this includes molar
89 flows, reactions, and an accumulation term ($\frac{dn_i}{dt} = (n_i)_{in} - (n_i)_{out} - (n_i)_{rxn}$).
90 Model structure may also include constraints such as fixed gain ratios, con-
91 straints on compositions, or other bounds that reflect physical realism. De-
92 tailing the full range of potential model structures is outside the scope of this
93 document. Equation 1 is a statement of a general model form that may include

94 differential, algebraic, continuous, binary, and integer variables.

$$0 = f\left(\frac{dx}{dt}, x, y, p, d, u\right) \quad (1a)$$

95 $0 = g(x, y, p, d, u) \quad (1b)$

96 $0 \leq h(x, y, p, d, u) \quad (1c)$

97 The solution of Equation 1 is determined by the initial state x_0 , a set of param-
98 eters p , a trajectory of disturbance values $d = (d_0, d_1, \dots, d_{n-1})$, and a sequence
99 of control moves $u = (u_0, u_1, \dots, u_{n-1})$. Likewise, the variables values may be
100 determined from the equations such as differential x or algebraic equations y .
101 The equations include differential f , algebraic g , and inequality constraints h .
102 The inequality constraints are included to model physical phenomena such as
103 phase changes where complementarity conditions are required. It is impor-
104 tant that the differential terms $\frac{dx}{dt}$ be expressed in implicit form as shown in
105 1a because some models cannot be rearranged into semi-explicit form such as
106 $\frac{dx}{dt} = f(x, y, p, d, u)$. With the methods for solving DAEs demonstrated in Sec-
107 tion 5, consistent initial conditions are not required and higher index DAEs are
108 solvable without differentiating the high index algebraic expressions [42]. An
109 example of this capability for both inconsistent initial conditions and high in-
110 dex DAEs is given by a pendulum application [43]. The pendulum equations of
111 motion are written as index-0 (ODE), index-1, index-2, and index-3 DAEs and
112 solvable with this approach. The drawback of this approach is that the problem
113 size is generally large, requiring the use of sparse methods and highly efficient
114 solvers. Also, a suitable initial guess for the state trajectories is often required
115 for solver convergence.

116 To implement Equation 1 within the APMonitor Modeling Language, the
117 following sections are defined with example values for each of the constants,
118 parameters, variables, intermediates, and equations as shown in Listing 1. In
119 the above example, values are defined with optional constraints and initial con-
120 ditions. The sample model describes a simple objective function $\min(x - 5)^2$
121 and a linear, first-order equation $\tau \frac{dx}{dt} = -x + y$ that dynamically relates the
122 input y to the output x . The intermediate variable y is defined as $y = Ku$
123 to simplify the implicit expression below. The above model is of no specific practi-
124 cal importance but is used to demonstrate the modeling format for differential
125 and algebraic equations. The model is compiled at run-time to provide sparse
126 first and second derivatives of the objective function and equations to solvers
127 through well-known automatic differentiation techniques [44].

128 3. Nonlinear Dynamic Estimation

129 Along with model form, the objective function is important to ensure desir-
130 able results. A common objective form is the least squares form: $(y_{model} - y_{measured})^2$
131 (see Equation 2). Although intuitive and simple to implement, the squared error
132 form has a number of challenges such as sensitivity to bad data or outliers. The

Listing 1: First Order Linear Model in APMonitor

```

Model
% Values that remain constant
Constants
    K = 2                % Model Constant
End Constants

% Values specified by the user or optimizer
Parameters
    tau = 2, >= 1, <= 10 % Model Parameter
    u   = 3, <= 100      % Manipulated Variable
End Parameters

% Implicitly solved variables
Variables
    x                % Controlled Variable
End Variables

% Explicit definition of temporary variables
Intermediates
    y = K * u        % Define Variable and Equation
End Intermediates

% Inequalities, equalities, algebraic or differential equations
Equations
    tau * $x = -x + y % First-order differential equation
End Equations
End Model

```

133 sensitivity to outliers is exacerbated by the squared error objective, commonly
 134 proposed for dynamic data reconciliation [45] [46] [47] [48] [49].

135 Table 1 details the equations of the typical squared error norm and the ℓ_1 -
 136 norm objective. The ℓ_1 -norm formulation in Equation 3 is less sensitive to data
 137 outliers and adjusts parameter values only when measurements are outside of a
 138 noise dead-band. A small penalty on Δp (change in the parameter values) also
 139 discourages parameter movement without sufficient improvement in the model
 140 predictions. The change can be from an initial guess or the prior estimates from
 141 a Moving Horizon Estimation (MHE) approach. The ℓ_1 -norm is similar to an
 142 absolute value function but is instead formulated with inequality constraints
 143 and slack variables. The absolute value operator is not continuously differen-
 144 tiable which can cause convergence problems for Nonlinear Programming (NLP)
 145 solvers. On the other hand, the ℓ_1 -norm slack variables and inequalities create
 146 an objective function that is smooth and continuously differentiable. Without
 147 the dead-band ($db = 0$) in Equation 3, the equations for c_U , c_L are not required
 148 and the form reduces to the commonly known ℓ_1 -norm for estimation that has
 149 desirable performance for outlier elimination [50] [51] [52] [53] [54] [55].

150 Pseudo-random binary signals (PRBS) are a popular technique to generate
 151 linear plant response models from data [56]. The example problem in Section
 152 6.1 demonstrates that PRBS-generated data can be used to determine optimal
 153 parameters for nonlinear dynamic models as well. Another technique for fit-
 154 ting model parameters to process data is the use of multiple steady-state data

Table 1: Estimation: Two Forms for Dynamic Data Reconciliation

Estimation with a Squared Error Objective

$$\begin{aligned}
 \min_{x,y,p,d} \quad & \Phi = (y_x - y)^T W_m (y_x - y) + \Delta p^T c_{\Delta p} + (y - \hat{y})^T W_p (y - \hat{y}) \\
 \text{s.t.} \quad & 0 = f\left(\frac{dx}{dt}, x, y, p, d, u\right) \\
 & 0 = g(x, y, p, d, u) \\
 & 0 \leq h(x, y, p, d, u)
 \end{aligned} \tag{2}$$

Estimation with an ℓ_1 -norm Objective with Dead-band

$$\begin{aligned}
 \min_{x,y,p,d} \quad & \Phi = w_m^T (e_U + e_L) + w_p^T (c_U + c_L) + \Delta p^T c_{\Delta p} \\
 \text{s.t.} \quad & 0 = f\left(\frac{dx}{dt}, x, y, p, d, u\right) \\
 & 0 = g(x, y, p, d, u) \\
 & 0 \leq h(x, y, p, d, u) \\
 & e_U \geq y - y_x + \frac{db}{2} \\
 & e_L \geq y_x - \frac{db}{2} - y \\
 & c_U \geq y - \hat{y} \\
 & c_L \geq \hat{y} - y \\
 & e_U, e_L, c_U, c_L \geq 0
 \end{aligned} \tag{3}$$

Nomenclature for Equations 2 and 3

Φ	objective function
y_x	measurements $(y_{x,0}, \dots, y_{x,n})^T$
y	model values $(y_0, \dots, y_n)^T$
\hat{y}	prior model values $(\hat{y}_0, \dots, \hat{y}_n)^T$
w_m, W_m	measurement deviation penalty
w_p, W_p	penalty from the prior solution
$c_{\Delta p}$	penalty from the prior parameter values
db	dead-band for noise rejection
x, u, p, d	states (x), inputs (u), parameters (p), or unmeasured disturbances (d)
Δp	change in parameters
f, g, h	equation residuals, output function, and inequality constraints
e_U, e_L	slack variable above and below the measurement dead-band
c_U, c_L	slack variable above and below a previous model value

155 sets [57]. Control engineers identify steady-state periods that cover the major
156 process operating regions of interest. One of the drawbacks to fitting a model
157 with steady-state data is that dynamic parameters cannot be fit from the data.
158 Dynamic parameters are those values that are multiplied by the derivatives
159 with respect to time in the equations. In the case of a linear first order sys-
160 tem $\left(\tau \frac{dy}{dt} = -y + Ku\right)$ the dynamic parameter is τ . However, process time
161 constants can typically be estimated from process fundamentals such as vessel
162 holdups and flow rates. In many cases, the time constants can be approximated
163 reasonably well. However, using only steady-state data for fitting parameters
164 can limit the observability of certain parameters that can only be determined
165 with dynamic data. If nonlinear MPC is to be used to the full potential, dynamic
166 data must be used to fit the models.

167 Using dynamic data to fit nonlinear dynamic models has a number of chal-
168 lenges. One of the challenges with the simultaneous solution approach is that
169 the data reconciliation problem can be very large. The data reconciliation prob-
170 lem is large because a discretization point of the DAE model must be calculated
171 at every time instant where a measurement is available. Using the simultaneous
172 optimization of model and objective function, the number of model states at
173 a particular time is multiplied by the number of time steps in the prediction
174 horizon. On the other hand, the sequential solution approach (solving objec-
175 tive function and model equations successively) reduces the number of variables
176 that must be solved simultaneously [58]. This approach is better suited to sys-
177 tems that have a small number of decision variables yet large number of model
178 variables or a long time horizon.

179 Other challenges in aligning the model to measured values include lack of
180 data diversity to obtain certain constants or co-linearity of parameters. The
181 sensitivity of parameters to the objective function can help guide which param-
182 eters have a significant effect on the outcome [59]. One solution to automatically
183 eliminate parameters with little sensitivity to the objective is to impose a small
184 penalty on parameter movement from a nominal value [60]. This approach au-
185 tomatically prevents unnecessary movement of parameter values that have little
186 effect on the results of the parameter estimation.

187 4. Nonlinear Control and Optimization

188 There are many challenges to the application of DAEs directly in nonlinear
189 control and optimization [61]. Recent advances include simultaneous methods
190 [58], decomposition methods [62] [63], efficient nonlinear programming solvers
191 [24], improved estimation techniques [64] [65] [66] [67], and experience with
192 applications to industrial systems [60] [68]. In particular, applications require
193 high service availability, reasonable extrapolation to operating conditions out-
194 side the original training set, and explanatory tools that reveal the rationale
195 of the optimization results. Other motivating factors include consideration of
196 lost opportunity during application development, sustainability of the solution,
197 and ease of development and maintenance by engineers without an advanced

198 training. In many instances non-technical challenges such as equipment and
 199 base-control reliability, operator training, and management support are critical
 200 factors in the success of an application [27].

201 A common objective function form is the squared error or ℓ_2 -norm objec-
 202 tive (see Equation 4). In this form, there is a squared penalty for deviation
 203 from a setpoint or desired trajectory. The squared error objective is simple to
 204 implement, has a relatively intuitive solution, and is well suited for Quadratic
 205 Programming (QP) or Nonlinear Programming (NLP) solvers.

206 An alternative form of the objective function is the ℓ_1 -norm objective (see
 207 Equation 5) that has a number of advantages over the squared error form similar
 208 to those discussed for the estimation case. For control problems, the advantage is
 209 not in rejection of outliers but in the explicit prioritization of control objectives.
 210 The ℓ_1 -norm simultaneously optimizes multiple objectives in one optimization
 211 problem as the solver manipulates the degrees of freedom selectively for the
 212 objective function contributions that have the highest sensitivity. Lower ranking
 213 objectives are met as degrees of freedom remain. However, the best objective
 214 function will always be met by minimizing the error associated with high ranking
 215 objectives. For problems that have safety, environmental, economic, and other
 216 competing priorities, the ℓ_1 -norm with a dead-band gives an intuitive form that
 217 manages these trade-offs as shown in Figure 1.

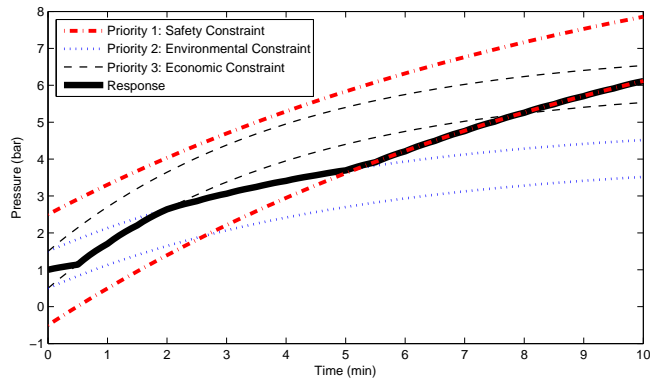


Figure 1: Competing priorities with safety, environmental, and economic ranges.

218 Priorities are assigned by giving the highest weighting (w_{hi}, w_{lo}) to the most
 219 important objectives. For the hypothetical pressure control example in Figure
 220 1 the safety constraint is never violated (highest priority). The economic target
 221 (lowest priority) is only satisfied when the other constraints are also satisfied
 222 from 0-2 minutes and drives the response along the upper limit of the envi-
 223 ronmental constraint from 2-5 minutes. When the environmental constraint
 224 (second highest priority) is violated, the response is driven to the lower limit of
 225 the safety constraint to have the least penalty for the environmental violation
 226 from 5-10 minutes. This dead-band also gives flexibility to have non-symmetric

227 objective functions in cases where an upper or lower limit is more important.
 228 Table 2 details the square error and ℓ_1 -norm objective functions.

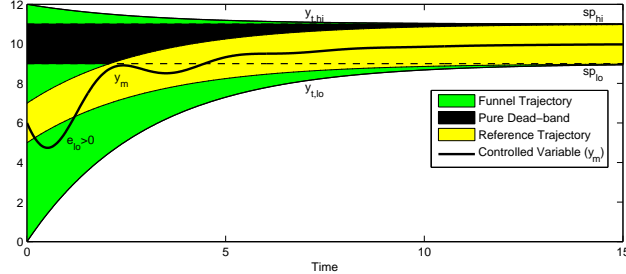


Figure 2: Three examples of ℓ_1 -norm dead-band trajectory regions for model predictive control.

229 The reference trajectories in both the squared-error and ℓ_1 -norm moderate
 230 the speed at which the controller attempts to reach the desired setpoint sp or
 231 reach the desired range sp_{lo}, sp_{hi} as shown in Figure 2. Three different ℓ_1 -
 232 norm trajectories are shown with varying initial conditions and are classified
 233 as a reference trajectory (inner-most), a pure dead-band (constant band), and
 234 a funnel trajectory (widest at the beginning). The initial conditions for $y_{t,hi}$
 235 and $y_{t,lo}$ adjust the starting positions of the reference trajectory region of no
 236 penalty. For dead-band control, the initial conditions are set to the final target
 237 values with $y_{t,hi} = sp_{hi}$ and $y_{t,lo} = sp_{lo}$. If restrictions on near-term dynamics
 238 are less important than reaching a target steady-state value, the gap between
 239 $y_{t,hi}$ and $y_{t,lo}$ can be made large relative to the range of the final dead-band
 240 sp_{hi} and sp_{lo} as shown by the funnel trajectory in Figure 2.

241 5. Numerical Solution of DAE Systems

242 Two types of methods for solving nonlinear MPC and dynamic optimization
 243 problems include sequential methods and simultaneous methods [58]. With the
 244 more compact sequential approach, the model equations are repeatedly solved
 245 to convergence tolerance to provide an objective function and gradient. The su-
 246 pervisory layer then proposes new decision variables and the simulation process
 247 is repeated. Conversely, the simultaneous approach involves solving the model
 248 equations and optimizing the objective function in parallel.

249 Sequential methods are easier to implement, but may fail to converge in a
 250 reasonable time for problems with a large number of degrees of freedom, thus
 251 delivering sub-optimal solutions. However, because sequential methods solve
 252 the model equations by forward integration, the solutions are always feasible
 253 with respect to the dynamic model, if not optimal. The simultaneous solution
 254 approach may be advantageous for certain problems, especially boundary value
 255 problems, terminal time constraints, and systems with unstable modes [42]. Si-
 256 multaneous optimization approaches generally have a computational advantage

Table 2: Control: Two Objective Forms for Nonlinear Dynamic Optimization

Control Squared Error Objective

$$\begin{aligned}
 \min_{x,y,u} \Phi &= (y - y_t)^T W_t (y - y_t) + y^T c_y + u^T c_u + \Delta u^T c_{\Delta u} \\
 \text{s.t.} \quad 0 &= f\left(\frac{dx}{dt}, x, y, p, d, u\right) \\
 &0 = g(x, y, p, d, u) \\
 &0 \leq h(x, y, p, d, u) \\
 \\
 \tau_c \frac{dy_t}{dt} + y_t &= sp
 \end{aligned} \tag{4}$$

Control ℓ_1 -norm Objective

$$\begin{aligned}
 \min_{x,y,u} \Phi &= w_{hi}^T e_{hi} + w_{lo}^T e_{lo} + y^T c_y + u^T c_u + \Delta u^T c_{\Delta u} \\
 \text{s.t.} \quad 0 &= f\left(\frac{dx}{dt}, x, y, p, d, u\right) \\
 &0 = g(x, y, p, d, u) \\
 &0 \leq h(x, y, p, d, u) \\
 \\
 \tau_c \frac{dy_{t,hi}}{dt} + y_{t,hi} &= sp_{hi} \\
 \tau_c \frac{dy_{t,lo}}{dt} + y_{t,lo} &= sp_{lo} \\
 e_{hi} &\geq y - y_{t,hi} \\
 e_{lo} &\geq y_{t,lo} - y
 \end{aligned} \tag{5}$$

Nomenclature for Equations 4 and 5

Φ	objective function
y	model values $(y_0, \dots, y_n)^T$
$y_t, y_{t,hi}, y_{t,lo}$	desired trajectory target or dead-band
w_{hi}, w_{lo}	penalty outside trajectory dead-band
$c_y, c_u, c_{\Delta u}$	cost of y, u and Δu , respectively
u, x, p, d	inputs (u), states (x), parameters (p), and disturbances (d)
f, g, h	equation residuals (f), output function (g), and inequality constraints (h)
τ_c	time constant of desired controlled variable response
e_{lo}, e_{hi}	slack variable below or above the trajectory dead-band
sp, sp_{lo}, sp_{hi}	target, lower, and upper bounds to final set-point dead-band

257 for control problems with many decision variables but with a moderate number
 258 of state variables. Sequential approaches may have computational advantage for
 259 a small number of decision variables coupled with large-scale models. Typical
 260 cases of large-scale models are distributed parameter systems. In this case, the
 261 computational gain obtained through simultaneous methods from the elimina-
 262 tion of repeated integration is overcome by the very large number of space and
 263 time discretized states.

264 A characteristic of the simultaneous problem formulation is that a general
 265 DAE model can be posed in open equation format (refer to Equation 1). In
 266 open equation format, DAE models of index-1 or higher are solved without re-
 267 arrangement or differentiation. The values of certain parameters, disturbances,
 268 or decision variables are discrete values over the time horizon to make the prob-
 269 lem tractable for numerical solution (e.g. MVs in Figure 3). On the other hand,
 270 integrated variables are determined from differential and algebraic equations
 and generally have a continuous profile (e.g. CVs in Figure 3). One solution

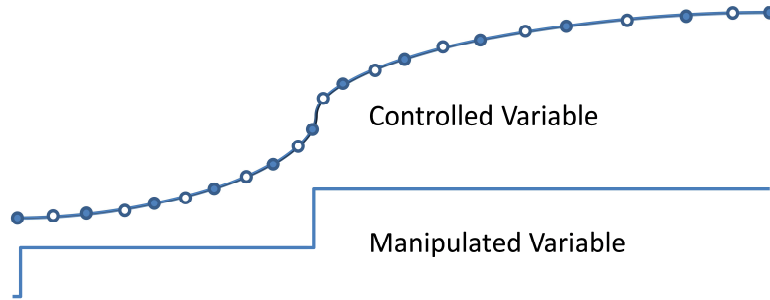


Figure 3: Dynamic equations are discretized over a time horizon and solved simultaneously. The solid nodes depict starting and ending locations for local polynomial approximations that are pieced together over the time horizon. With one internal node for each segment, this example uses a 2nd order polynomial approximation for each step.

271 approach to this dynamic system is the conversion of the DAE system to algebraic
 272 equations through direct transcription [14]. This technique is also known
 273 as orthogonal collocation on finite elements [69]. Converting the DAE system
 274 to a Nonlinear Programming (NLP) problem permits the solution by large-scale
 275 solvers [46] [70]. Additional details of the simultaneous approach are shown in
 276 Section 5.1 and an example problem in Section 5.2.

278 5.1. Weighting Matrices for Orthogonal Collocation

279 The objective is to determine a matrix M that relates the derivatives to the
 280 non-derivative values over a horizon at points $1, \dots, n$ as shown in Equation 6.
 281 In the case of Equation 6, four points are shown for the derivation. The initial
 282 value, x_0 , is a fixed initial condition or otherwise equal to the final point from

283 the prior interval.

$$\begin{bmatrix} \dot{x}_1 \\ \dot{x}_2 \\ \dot{x}_3 \end{bmatrix} = M \left(\begin{bmatrix} x_1 \\ x_2 \\ x_3 \end{bmatrix} - \begin{bmatrix} x_0 \\ x_0 \\ x_0 \end{bmatrix} \right) \quad (6)$$

284 The solution of the differential equations at discrete time points is approximated
285 by a Lagrange interpolating polynomial as shown in Equation 7.

$$x(t) = A + Bt + Ct^2 + Dt^3 \quad (7)$$

286 Time points for each interval are chosen according to Lobatto quadrature. All
287 time points are shifted to a reference time of zero ($t_0 = 0$) and a final time of
288 $t_n = 1$. For 3 nodes per horizon step, the one internal node is chosen at $t_1 = \frac{1}{2}$.
289 An example of internal nodes are displayed in Figure 3 where the horizon is
290 broken into multiple intervals of Lobatto quadrature with 3 nodes per horizon
291 step (one internal node). In the case of 4 nodes per horizon step, the internal
292 values are chosen at $t_1 = \frac{1}{2} - \frac{\sqrt{5}}{10}$ and $t_2 = \frac{1}{2} + \frac{\sqrt{5}}{10}$. With 5 nodes, time values are
293 $\frac{1}{2} - \frac{\sqrt{21}}{14}$, $\frac{1}{2}$, and $\frac{1}{2} + \frac{\sqrt{21}}{14}$. At 6 nodes, time values are $\frac{1}{2} - \frac{\sqrt{7+2\sqrt{7}}}{42}$, $\frac{1}{2} - \frac{\sqrt{7-2\sqrt{7}}}{42}$,
294 $\frac{1}{2} + \frac{\sqrt{7-2\sqrt{7}}}{42}$, and $\frac{1}{2} + \frac{\sqrt{7+2\sqrt{7}}}{42}$.

295 In this derivation, a third-order polynomial approximates the solution at the
296 four points in the horizon. Increasing the number of collocation points increases
297 the corresponding polynomial order. For initial value problems, the coefficient A
298 is equal to x_0 , when the initial time is arbitrarily defined as zero. To determine
299 the coefficients B , C , and D , Equation 7 is differentiated and substituted into
300 Equation 6 to give Equation 8. Note that the A coefficient from Equation 7 is
301 cancelled by x_0 on the right-hand side of Equation 8.

$$\begin{bmatrix} B + 2Ct_1 + 3Dt_1^2 \\ B + 2Ct_2 + 3Dt_2^2 \\ B + 2Ct_3 + 3Dt_3^2 \end{bmatrix} = M \begin{bmatrix} Bt + Ct_1^2 + Dt_1^3 \\ Bt + Ct_2^2 + Dt_2^3 \\ Bt + Ct_3^2 + Dt_3^3 \end{bmatrix} \quad (8)$$

$$\begin{bmatrix} 1 & 2t_1 & 3t_1^2 \\ 1 & 2t_2 & 3t_2^2 \\ 1 & 2t_3 & 3t_3^2 \end{bmatrix} \begin{bmatrix} B \\ C \\ D \end{bmatrix} = M \begin{bmatrix} t_1 & t_1^2 & t_1^3 \\ t_2 & t_2^2 & t_2^3 \\ t_3 & t_3^2 & t_3^3 \end{bmatrix} \begin{bmatrix} B \\ C \\ D \end{bmatrix}$$

302 Finally, rearranging and solving for M gives the solution shown in Equation 9.

$$M = \begin{bmatrix} 1 & 2t_1 & 3t_1^2 \\ 1 & 2t_2 & 3t_2^2 \\ 1 & 2t_3 & 3t_3^2 \end{bmatrix} \begin{bmatrix} t_1 & t_1^2 & t_1^3 \\ t_2 & t_2^2 & t_2^3 \\ t_3 & t_3^2 & t_3^3 \end{bmatrix}^{-1} \quad (9)$$

303 The final form that is implemented in practice is shown in Equation 10 by
304 inverting M and factoring out the final time t_n ($t_n N = M^{-1}$). This form
305 improves the numerical characteristics of the solution, especially as the time
306 step approaches zero ($t_n \rightarrow 0$).

$$t_n N \begin{bmatrix} \dot{x}_1 \\ \dot{x}_2 \\ \dot{x}_3 \end{bmatrix} = \begin{bmatrix} x_1 \\ x_2 \\ x_3 \end{bmatrix} - \begin{bmatrix} x_0 \\ x_0 \\ x_0 \end{bmatrix} \quad (10)$$

307 The matrices that relate $\frac{dx}{dt}$ to x are given in Tables A.6 and A.7 in Appendix
 308 A for intervals with 3 to 6 nodes.

309 5.2. Example Solution by Orthogonal Collocation

310 A simultaneous solution demonstrates the application of orthogonal collocation.
 311 In this case, the first order system $\tau \frac{dx}{dt} = -x$ is solved at 6 points
 312 from $t_0 = 0$ to $t_n = 10$ using Equation A.4. In this case $\tau = 5$ and the initial
 313 condition is specified at $x_0 = 1$. For this problem, the time points for $\frac{dx}{dt}$ and x
 314 are selected as 0, 1.175, 3.574, 6.426, 8.825, and 10. The value of x is specified
 315 at $t_0 = 0$ due to the initial condition. As a first step, equations for $\frac{dx}{dt}$ are
 316 generated in Equation 11.

$$\frac{dx}{dt} = \begin{bmatrix} \dot{x}_1 \\ \dot{x}_2 \\ \dot{x}_3 \\ \dot{x}_4 \\ \dot{x}_5 \end{bmatrix} = (t_n N_{5x5})^{-1} \left(\begin{bmatrix} x_1 \\ x_2 \\ x_3 \\ x_4 \\ x_5 \end{bmatrix} - \begin{bmatrix} x_0 \\ x_0 \\ x_0 \\ x_0 \\ x_0 \end{bmatrix} \right) \quad (11)$$

317 Substitution of Equation 11 into the derivatives of the model equation yields
 318 a linear system of equations as shown in Equation 12.

$$\tau \frac{dx}{dt} = -x$$

$$\tau (t_n N_{5x5})^{-1} \left(\begin{bmatrix} x_1 \\ x_2 \\ x_3 \\ x_4 \\ x_5 \end{bmatrix} - \begin{bmatrix} x_0 \\ x_0 \\ x_0 \\ x_0 \\ x_0 \end{bmatrix} \right) = - \begin{bmatrix} x_1 \\ x_2 \\ x_3 \\ x_4 \\ x_5 \end{bmatrix} \quad (12)$$

319 Equation 12 is rearranged and solved with linear algebra as shown in Equa-
 320 tion 13.

$$\begin{bmatrix} x_1 \\ x_2 \\ x_3 \\ x_4 \\ x_5 \end{bmatrix} = \left(\tau (t_n N_{5x5})^{-1} + I \right)^{-1} \tau (t_n N_{5x5})^{-1} \begin{bmatrix} x_0 \\ x_0 \\ x_0 \\ x_0 \\ x_0 \end{bmatrix} = \begin{bmatrix} 0.791 \\ 0.489 \\ 0.277 \\ 0.171 \\ 0.135 \end{bmatrix} \quad (13)$$

321 The numerical solution given in Equation 13 is within three significant figures
 322 of the analytical solution $x(t) = x_0 e^{-\frac{t}{\tau}}$, verifying that the numerical solution
 323 approximations are sufficiently accurate in this case. This is not always the case
 324 and discretization must sometimes be refined to reduce numerical error.

325 6. Application: Quadruple Tank Level Control

326 A quadruple tank process shown in Figure 4 has been the subject of the-
 327 oretical [71] and practical demonstrations [72] [73] [74] [75] of a multivariable

328 and highly coupled system [73]. The four tank process has also been a test
 329 application for application of decentralized and coordinated control techniques
 330 [76] [77]. A number of other interesting characteristics of this process include
 331 configurations that cause the system to go unstable. This can be observed by
 332 showing that there are unstable poles in a transfer function representation of
 333 the system. Another challenge is the nonlinear tendency of the system. For
 334 example, this can be characterized by variable gains of the MVs to the CVs.

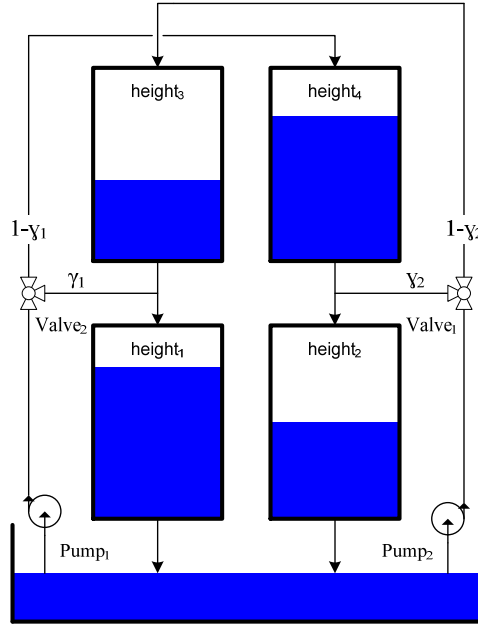


Figure 4: Diagram of the quadruple tank process. Pump 1 supplies tanks 1 and 4 while pump 2 supplies tanks 2 and 3.

335 The four tank process has two pumps that are adjusted with variable voltage
 336 to pump 1 (v_1) and pump 2 (v_2). A fraction of water from pump 1 is diverted
 337 to tank 1 proportional to γ_1 and to tank 4 proportional to $(1 - \gamma_1)$. Similarly,
 338 a fraction of water from pump 2 is diverted to tank 2 proportional to γ_2 and
 339 to tank 3 proportional to $(1 - \gamma_2)$. The valves that determine γ_1 and γ_2 are
 340 manually adjusted previous to the experiment and are held constant through-
 341 out a particular period of data collection. All tanks are gravity drained and
 342 tank 3 outlet enters tank 1. Tank 4 outlet enters tank 2, creating a coupled
 343 system of MVs and CVs. For $(\gamma_1 + \gamma_2) \in (0, 1)$, the linearized system has no
 344 RHP zeros with for $(\gamma_1 + \gamma_2) \in (1, 2)$, the linearized system has one RHP zero
 345 [71]. A RHP zero indicates that there may either be overshoot or an inverse
 346 response to a step change in the MV.

347 A combination of material balances and Bernoulli's law yields the process
 348 model for the four tank process as shown in Equation 14. The equations are

349 also displayed in Appendix B in the APMonitor Modeling Language.

$$\begin{aligned} q_a &= k_m v_1 + k_b \\ q_b &= k_m v_2 + k_b \end{aligned} \quad (14a)$$

350

$$\begin{aligned} q_{1,in} &= \gamma_1 q_a + q_{3,out} \\ q_{2,in} &= \gamma_2 q_b + q_{4,out} \\ q_{3,in} &= (1 - \gamma_2) q_b \\ q_{4,in} &= (1 - \gamma_1) q_a \end{aligned} \quad (14b)$$

351

$$\begin{aligned} q_{1,out} &= c_1 \sqrt{2gh_1} \\ q_{2,out} &= c_2 \sqrt{2gh_2} \\ q_{3,out} &= c_3 \sqrt{2gh_3} \\ q_{4,out} &= c_4 \sqrt{2gh_4} \end{aligned} \quad (14c)$$

352

$$\begin{aligned} A_1 \frac{dh_1}{dt} &= q_{1,in} - q_{1,out} \\ A_2 \frac{dh_2}{dt} &= q_{2,in} - q_{2,out} \\ A_3 \frac{dh_3}{dt} &= q_{3,in} - q_{3,out} \\ A_4 \frac{dh_4}{dt} &= q_{4,in} - q_{4,out} \end{aligned} \quad (14d)$$

353 where γ_1 is the split factor for tanks 1 and 4 and γ_2 is the split factor leading
 354 to tanks 2 and 3 and the range of allowable values is $0 \leq \gamma_i \leq 1$. When $\gamma_i = 0$
 355 all of the flow from the pumps enters the top tanks (3 or 4) and when $\gamma_i = 1$ all
 356 of the flow enters the lower tanks (1 or 2). The other parameters for this model
 357 include c_i as the outflow factor for tank i , k_m as the valve linearization slope, k_b
 358 as the valve linearization intercept, and A_i as the cross-sectional area of tank i .
 359 The variables include q_a as the flow from pump 1, q_b as the flow from pump 2,
 360 $q_{i,in}$ as the inlet flow to tank i , $q_{i,out}$ as the outlet flow from tank i , and h_i as
 361 the height of liquid in tank i .

362 Equation set 14a is the relationship between pump voltage and flow while
 363 Equation set 14b defines the inlet flow to each of the tanks. Equation set 14c
 364 is the outlet flow from each of the tanks with tanks 3 and 4 draining to tanks
 365 1 and 2, respectively. Finally, equation set 14d is a material balance around
 366 each tank with accumulation, inlet, and outlet terms. In this case, the density
 367 is assumed to be constant allowing a volumetric balance to be used instead.

368 The process model is nonlinear because the outlet flow is proportional to the
 369 square root of the liquid level. In this experiment, tanks 1 and 3 and tanks 2
 370 and 4 have the same outlet diameter making $c_1 = c_3$ and $c_2 = c_4$. Additionally,
 371 tanks 1 and 3 have a cross-sectional area of 28 cm² while tanks 2 and 4 have a
 372 cross-sectional area of 32 cm². Unknown parameters include γ_1 , γ_2 , $c_{1,3}$, $c_{2,4}$,
 373 k_m , and k_b . The unknown parameters are determined from dynamic data.

374 *6.1. Quadruple Tank Parameter Estimation*

375 For the quadruple tank process, the model has only 14 differential or al-
 376 gebraic states. When calculated over the PRBS data horizon, the resulting
 377 optimization problem has 5766 to 11,526 variables, depending on the objective
 378 function form. There are additional equations for the differential states in the
 379 optimization problem from the orthogonal collocation transformation (see Sec-
 380 tion 5). Direct transcription by orthogonal collocation on finite elements is one
 381 of the methods to convert DAE systems into a Nonlinear Programming (NLP)
 382 problem [78]. This is accomplished by approximating time derivatives of the
 383 DAE system as algebraic relationships as discussed previously. Figure 5 shows
 384 the results of the reconciliation to the PRBS-generated data.

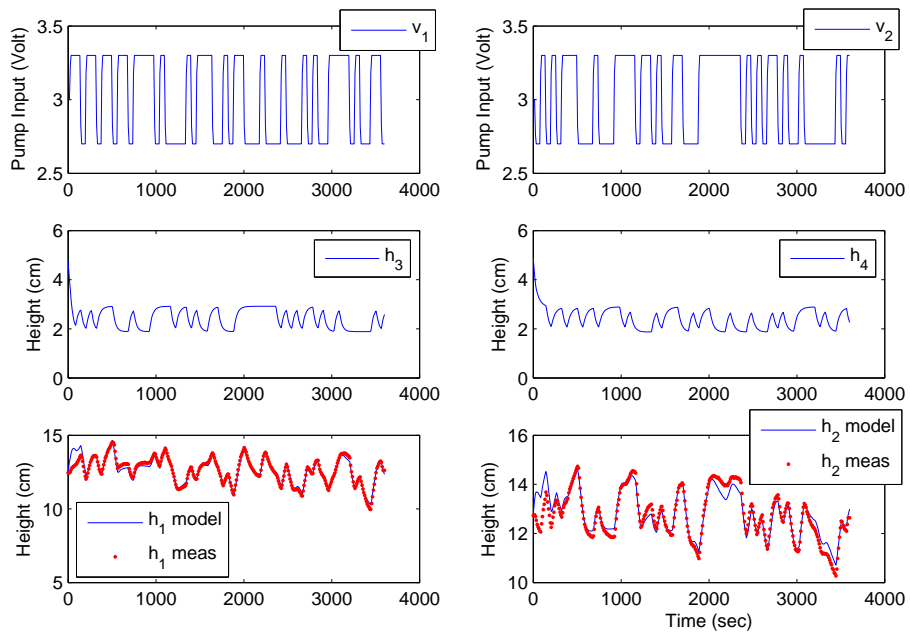


Figure 5: Results of the dynamic parameter estimation using PRBS generated data.

385 Only levels for tanks 1 and 2 are measured as shown in Figure 5. For the
 386 quadruple tank process 6 parameters were estimated, namely γ_1 , γ_2 , $c_{1,3}$, $c_{2,4}$,
 387 k_m , and k_b . The optimization solution overview is shown in Table 3 while
 388 initial and final values of the parameters are displayed in Table 4. MATLAB and
 389 Python scripts for configuring and solving this problem are shown in Listing 3
 390 of Appendix C. The MATLAB or Python scripts use the APMonitor Modeling
 391 Language [15] model (see Appendix B) to create the differential and algebraic
 392 (DAE) model. APMonitor translates the problem into an NLP and solves the
 393 equations with one of many large-scale solvers. The particular solver used in this

394 study is IPOPT, an interior point large-scale nonlinear programming solver [24],
 395 for solving the resulting optimization problem. A summary of the optimization
 396 problem and the solution is shown in Table 3.

Table 3: Summary of the Dynamic Data Reconciliation

Optimization Problem Overview		
Description	ℓ_1 -Norm	Squared Error
Iterations	33	10
CPU Time (2.5 GHz Intel i7 Processor)	32.5 sec	10.3 sec
Number of Variables	11,526	5,766
Number of Equations	11,520	5,760
Degrees of Freedom	6	6
Number of Jacobian Non-zeros	40,312	28,792

397 Using different objective function forms resulted in similar parameter estimates
 398 and comparable model predictions. As seen in Table 4, the optimal
 399 values for the parameters were well within the upper and lower constraints.
 400 These constraints were set for both ℓ_1 -norm and squared-error problems based
 401 on knowledge of the process; a violation of these constraints would indicate un-
 402 reasonable parameter values. In this case, the ℓ_1 -norm optimization problem
 403 had roughly twice the number of variables and required 3 times the amount of
 404 CPU time to find a solution. In this case, the increased computational time is
 405 an additional cost associated with ℓ_1 -norm estimation.

Table 4: Results of the Dynamic Data Reconciliation

Initial and Final Values of the Estimation Problem					
Parameter	Initial Value	Lower Bound	Upper Bound	ℓ_1 -Norm Results	Squared Error Results
γ_1	0.43	0.20	0.80	0.627	0.585
γ_2	0.34	0.20	0.80	0.591	0.548
$c_{1,3}$	0.071	0.010	0.200	0.0592	0.0630
$c_{2,4}$	0.057	0.010	0.200	0.0548	0.0582
k_m	10.0	3.0	20.0	3.543	3.444
k_b	0.00	-2.00	2.00	-1.675	-0.810

406 Improved outlier rejection and parameter estimates are shown by purpose-
 407 fully introducing corrupted data. Three cases are shown in Figure 6 with the
 408 corrupted data being introduced at 1200 seconds.

409 The first case of corrupted data is a single outlier that is 10 cm higher than
 410 the actual measured value. While this specific outlier could easily be removed

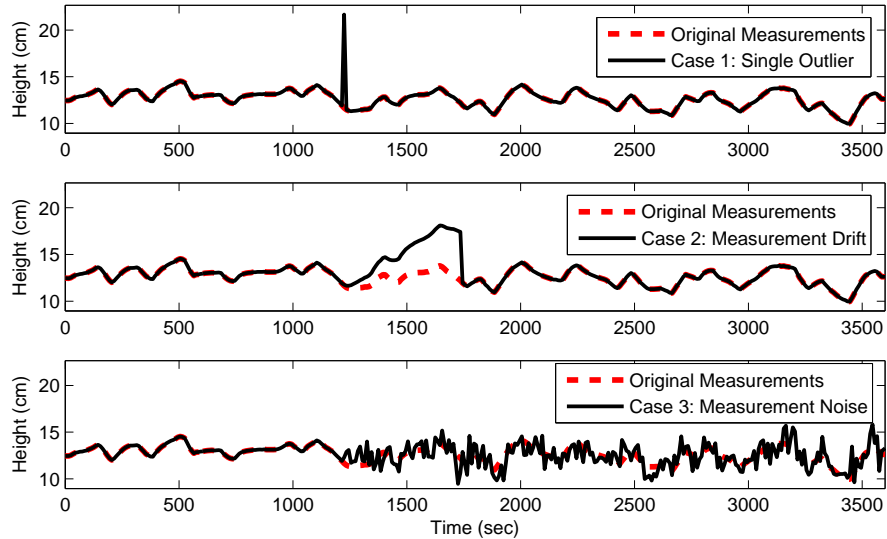


Figure 6: Three cases of corrupted data with (1) single outlier, (2) measurement drift, and (3) measurement noise.

411 by automated outlier detection, it may not be possible to eliminate all outliers
 412 from data especially for real-time or large-scale systems. A second case involves
 413 measurement drift at a rate of $+0.1$ cm per second. After 550 seconds, the
 414 measurement drift is corrected and the measurement returns to actual measured
 415 values. A third case introduces normally distributed measurement noise with
 416 zero mean and standard deviation of one.

417 For all cases, it is desirable to retain original parameters even in the presence
 418 of corrupted data. The ℓ_1 -norm form outperforms the squared-error form in two
 419 of the three cases and slightly better on the case with added noise. In the case of
 420 the single outlier, the ℓ_1 -norm parameter values do not change, demonstrating
 421 the value in rejecting outlier values. In the case of measurement drift, the ℓ_1 -
 422 norm error parameters change by from 0-2% while the squared-error parameters
 423 change between 3-37%. Finally, for the measurement noise case, the ℓ_1 -norm and
 424 squared-error parameters both change although the squared-error parameters
 425 change by roughly twice that of the ℓ_1 -norm parameters. This corrupted data
 426 example demonstrates the ability of the ℓ_1 -norm to better reject outliers, sensor
 427 drift, and noise.

428 6.2. Nonlinear Optimization of the Quadruple Tank System

429 Continuing with the quadruple tank example, the squared error model pa-
 430 rameters from Section 6.1 are used to update the model. Either the squared-
 431 error or the ℓ_1 -norm objective estimation values can be used because of nearly

Table 5: Changing Parameter Results with Corrupted Data

Parameter Value Change with ℓ_1 -norm						
	γ_1	γ_2	$c_{1,3}$	$c_{2,4}$	k_m	k_b
Case 1 (Outlier)	0%	0%	0%	0%	0%	0%
Case 2 (Drift)	1%	1%	2%	0%	1%	0%
Case 3 (Noise)	5%	2%	8%	4%	2%	21%
Parameter Value Change with Squared Error						
	γ_1	γ_2	$c_{1,3}$	$c_{2,4}$	k_m	k_b
Case 1 (Outlier)	11%	6%	3%	4%	6%	42%
Case 2 (Drift)	3%	11%	15%	5%	3%	37%
Case 3 (Noise)	9%	4%	2%	9%	7%	72%

432 equivalent results. Data reconciliation can either be performed once or repeat-
433 edly as new measurements arrive in a receding horizon approach. As new mea-
434 surements arrive, the model is readjusted to fit the data and continually refine
435 the model predictions. These updated parameters can then be used in the
436 NMPC application to better predict the future response.

437 Once the model is updated, nonlinear optimization calculates the optimal
438 trajectory of the MV. In this case, a future move plan of the voltage to the
439 two pumps is calculated as shown in Figure 7. MV moves are constrained by
440 change, upper, and lower limits. The change constraints are set to limit the
441 amount that the MV can move for each control action step and in this case
442 the move limit is set to $|\Delta MV| \leq 1$. With a cycle time of 1 second, the rate
443 that the voltage to the pump can change is $\pm 1 \frac{V}{sec}$. The control action is also
444 constrained by absolute minimum ($MV_L = 1$) and maximum ($MV_U = 6$) limits.
445 The lower limit is reached for the first pump ($v1$) and remains at the lower limit
446 for 30 seconds before settling at the steady state value at 1.41V. The upper
447 limit is reached for second pump ($v2$) within two steps into the horizon and
448 afterwards settles to a steady state value of 4.58V. This over-shoot or under-
449 shoot of MVs is typical for CV tuning that is faster than the natural process
450 time constant. The natural process time constant is the speed of response due
451 to a step change in a process input. When requesting a response that is faster
452 than this nominal step change, the MVs must over-react to move the process
453 faster. In most cases, steady state values of the MVs are independent of the
454 controller tuning. CV tuning is a critical element to achieving desirable control
455 performance. Aggressive CV tuning is shown in this example, giving over- or
456 under-shoot of the MVs. For CV tuning that is equal to the natural process
457 time constant, there will typically be a step to the new solution. For slower
458 CV tuning, the MV ramps to the steady state value. Other MPC ℓ_1 -norm
459 formulations have particular drawbacks that either lead to dead-beat or idle
460 control performance [79].

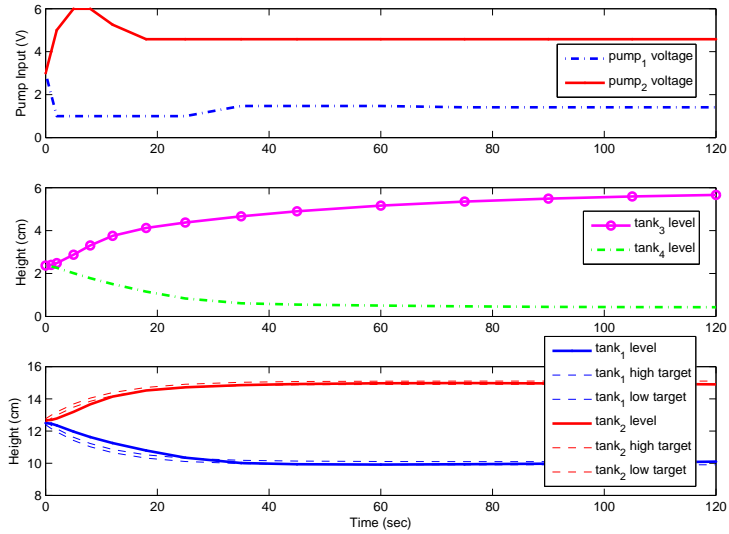


Figure 7: Model predictive control solution showing voltage input to the pumps 1 and 2.

461 There are many types of CV tuning options that are typical in linear or non-
 462 linear control applications. In this case, an ℓ_1 -norm with dead-band is demon-
 463 strated for the simulated controller. The speed of the CV response is dictated by
 464 an upper and lower first order reference trajectory with time constant τ_C . Only
 465 values that are outside this dead-band are penalized in the objective function.
 466 The form of this controller objective is desirable for minimizing unnecessary MV
 467 movement to achieve a controller objective. In this form, MV movement only
 468 occurs if the projected CV response is forecast to deviate from a pre-described
 469 range. The bottom subplot of Figure 7 displays the CV response along with the
 470 upper and lower trajectories that define the control objective.

471 7. Large-Scale Systems

472 The quadruple tank system is a small-scale system that has been included
 473 here and in many other benchmark studies to demonstrate control techniques
 474 for multi-variable systems. An additional example is the computational re-
 475 quirements for large-scale systems. A test of the scale-up of the simultaneous
 476 approach for optimization is presented here with varying problem sizes with a
 477 state space model. In particular, the number of MVs and CVs is varied to reveal
 478 computational time required to determine an optimal solution for a single cycle
 479 of the controller. The controller has a quadratic objective function and linear

480 constraints as shown in Equation 15.

$$\begin{aligned}
& \min_{x \in R^n, y \in R^p, u \in R^m} \Phi = (y - y_t)^T W_t (y - y_t) + y^T c_y + u^T c_u + \Delta u^T c_{\Delta u} \\
& \text{s.t. } \frac{dx}{dt} = Ax + Bu, \quad A = -I_{n \times n}, \quad B = \begin{bmatrix} 1 & \dots & 1 \\ 0 & \dots & 0 \\ \vdots & \ddots & \vdots \\ 0 & \dots & 0 \end{bmatrix}_{n \times m} \quad (15)
\end{aligned}$$

$$y = Cx + Du, \quad C = I_{p \times n}, \quad D = 0_{p \times m}$$

$$\tau_c \frac{dy_t}{dt} + y_t = sp$$

$$0 \leq u \leq 10$$

481

482 The number of MVs (m) and number of CVs (p) are adjusted to vary the
483 problem size. The controller is configured with $W_t = I_{p \times p}$, $c_y = c_u = c_{\Delta u} =$
484 $0_{m \times 1}$, $\tau_c = 1_{p \times 1}$, $sp = 1_{p \times 1}$, and initial condition $x_0 = 0_{n \times 1}$. Each of the
485 MVs affects each of the CVs, leading to a dense step response mapping. The
486 cycle time is assumed to be 6 seconds with a prediction horizon of 120 minutes.
487 The discretization times are chosen as 0, 0.1, 0.2, 0.4, 0.8, 1.5, 3, 6, 12, 25, 50,
488 60, 80, 100, and 120. The non-uniform time steps allow near-term resolution
489 for control action and long-term predictions for control target calculations. An
490 active set solver (APOPT) and an interior point solver (IPOPT) are tested for
491 the combination of MVs and CVs quantities as shown in Figure 8.

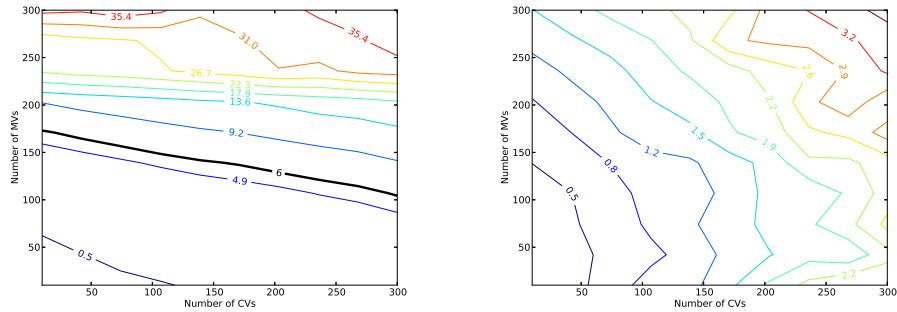


Figure 8: Contour plot of CPU times for varying numbers of MVs and CVs for APOPT and IPOPT, respectively.

492

493 The APOPT solver has excellent scaling with increased number of CVs but
494 poor computational scaling with increased number of MVs (decision variables).
495 This is expected from an active set solver where the basis selection and active set
496 switching requires intensive matrix operations. Once the correct set of active
497 constraints is determined, the algorithm can rapidly converge to an optimal
498 solution.

498 The largest case with 300 MVs and 300 CVs translates into an optimization
 499 problem with 12,600 variables, 8,400 equations, and 4,200 degrees of freedom
 500 (decision variables) because the equations are discretized over the time horizon.
 501 Others have also demonstrated large-scale MPC with an ℓ_1 -norm objective such
 502 a 400 MV/400 CV application to a paper machine cross direction control [80]
 503 [81]. The present case is solved in 3.8 sec with the IPOPT solver and in 39.5 sec
 504 with APOPT solver. A known advantage of interior point solvers is the excellent
 505 scaling with additional degrees of freedom. An advantage of active set solvers
 506 is the ability to quickly find a solution from a nearby candidate solution. A
 507 suggested approach is to use the interior point solver to initialize a problem and
 508 switch to an active set method for cycle-to-cycle cases that can be initialized
 509 from a prior solution.

510 8. Conclusions

511 This paper gives details on the implementation of nonlinear modeling, data
 512 reconciliation, and dynamic optimization. The examples relate the common
 513 steps typically deployed in linear MPC applications to a comparable procedure
 514 for nonlinear applications. As a foundation for using dynamic models, the
 515 process of converting differential equations into a set of algebraic equations is
 516 reviewed. This conversion step is necessary to solve the model and objective
 517 function simultaneously with NLP solvers. The application in this paper is the
 518 quadruple tank process that is a well-known example of multivariate control. As
 519 a first step, certain parameters of the model are adjusted to fit to PRBS data
 520 through dynamic data reconciliation. In a next step, the controller is tuned
 521 to provide desirable control responses for set point tracking and disturbance
 522 rejection. For both estimation and control cases, alternate squared error and
 523 ℓ_1 -norm error forms are compared. While the ℓ_1 -norm error uses additional
 524 variables and equations, it adds only linear equality and inequality constraints.
 525 Along with the overview, example MATLAB and Python scripts are given in the
 526 Appendix as a guide to implement the problems in the text. While this is not an
 527 exhaustive review of all available techniques or software, it provides a platform
 528 and case study to advance the use of nonlinear models in control research and
 529 practice.

530 Appendix A. Direct Transcription by Orthogonal Collocation on Fi- 531 nite Elements

532 The matrices that relate $\frac{dx}{dt}$ to x are given in Tables A.6 and A.7 for inter-
 533 vals with 3 to 6 nodes. The formula for 2 nodes reduces to Euler's method for
 534 numerical integration differential equations. However, in this case the equations
 535 are not solved sequentially in time but simultaneously by an implicit solution
 536 method. Additional accuracy can be achieved over one interval with more nodes
 537 but more nodes also increases the number of equations and size of the problem.
 538 The time dynamic horizon is typically divided over a number of intervals where

539 these equations are applied. An additional set of these equations must be in-
540 cluded for every differential variable that appears in the model equations. In
541 this case the differential variables are treated like regular algebraic variables
542 because there is an additional equation for every unknown derivative value at
543 every time point.

Table A.6: Direct Transcription to Solve Differential Equations as Sets of Algebraic Equations

Orthogonal Collocation Equations

$$t_n N_{2 \times 2} \begin{bmatrix} \dot{x}_1 \\ \dot{x}_2 \end{bmatrix} = \begin{bmatrix} x_1 \\ x_2 \end{bmatrix} - \begin{bmatrix} x_0 \\ x_0 \end{bmatrix} \quad (\text{A.1})$$

$$t_n N_{3 \times 3} \begin{bmatrix} \dot{x}_1 \\ \dot{x}_2 \\ \dot{x}_3 \end{bmatrix} = \begin{bmatrix} x_1 \\ x_2 \\ x_3 \end{bmatrix} - \begin{bmatrix} x_0 \\ x_0 \\ x_0 \end{bmatrix} \quad (\text{A.2})$$

$$t_n N_{4 \times 4} \begin{bmatrix} \dot{x}_1 \\ \dot{x}_2 \\ \dot{x}_3 \\ \dot{x}_4 \end{bmatrix} = \begin{bmatrix} x_1 \\ x_2 \\ x_3 \\ x_4 \end{bmatrix} - \begin{bmatrix} x_0 \\ x_0 \\ x_0 \\ x_0 \end{bmatrix} \quad (\text{A.3})$$

$$t_n N_{5 \times 5} \begin{bmatrix} \dot{x}_1 \\ \dot{x}_2 \\ \dot{x}_3 \\ \dot{x}_4 \\ \dot{x}_5 \end{bmatrix} = \begin{bmatrix} x_1 \\ x_2 \\ x_3 \\ x_4 \\ x_5 \end{bmatrix} - \begin{bmatrix} x_0 \\ x_0 \\ x_0 \\ x_0 \\ x_0 \end{bmatrix} \quad (\text{A.4})$$

544 Appendix B. Quadruple Tank Model

545 The quadruple tank process is represented by 14 differential and algebraic
546 equations (DAEs). The following model in Listing 2 is expressed in the APMon-
547 itor Modeling Language. This file and others included in the paper are available
548 at APMonitor.com as a MATLAB toolbox [82] or as a Python package [83].

549 Appendix C. Parameter Estimation with a PRBS-Generated Signal

550 The following MATLAB and Python scripts in Listing 3 detail the com-
551 mands necessary to reproduce the parameter estimation case presented in this
552 paper. The parameter estimation uses two elements including the model file
553 (4tank.apm) and a data file (prbs360.csv). The model file is shown in Appendix
554 B while the data file is available for download from APMonitor.com under the
555 MATLAB or Python example sections.

Listing 2: Four Tank Model in APMonitor

```

Model
  Constants
    % gravitational constant (cm/s^2)
    g = 981
    % tank cross-sectional area (cm^2)
    Area[1] = 28
    Area[2] = 32
    Area[3] = 28
    Area[4] = 32
    % relation of level to voltage measurement (V/cm)
    kc = 0.50
  End Constants

  Parameters
    % relation of input voltage to pump flow rate (cm^3/sec / V)
    km = 10.0, >=3.0, <=20.0 % slope
    kb = 0.0, >=-20.0, <=20.0 % intercept
    % correction factors to fit model to real data
    c13 = 0.071, >0.01, <=0.2 % outlet flow corrections
    c24 = 0.057, >0.01, <=0.2 % outlet flow corrections
    % fractional split to tank 1 vs. tank 4
    gamma[1] = 0.43, >=0, <=1
    % fractional split to tank 2 vs. tank 3
    gamma[2] = 0.34, >=0, <=1
    % voltage to pump A
    v1 = 3, >=0, <=10 % Volt
    % voltage to pump B
    v2 = 3, >=0, <=10 % Volt
  End Parameters

  Variables
    % tank height - diameter = 6 cm, max height = 20 cm
    h[1] = 12.6, >=1e-5
    h[2] = 13.0, >=1e-5
    h[3] = 4.8, >=1e-5
    h[4] = 4.9, >=1e-5
  End Variables

  Intermediates
    % correction factors
    c[1] = c13
    c[2] = c24
    c[3] = c13
    c[4] = c24
    % pump flows
    qa = v1 * km + kb
    qb = v2 * km + kb
    % inlet flows from pumps
    q[1] = gamma[1] * qa
    q[2] = gamma[2] * qb
    q[3] = (1-gamma[2]) * qb
    q[4] = (1-gamma[1]) * qa
    % outlet flows
    out[1:4] = c[1:4] * sqrt(2*g*h[1:4])
    % total inlet flows
    in[1] = q[1] + out[3]
    in[2] = q[2] + out[4]
    in[3] = q[3]
    in[4] = q[4]
  End Intermediates

  Equations
    Area[1:4] * $h[1:4] = in[1:4] - out[1:4] % $ = differential
  End Equations
End Model

```


Table A.7: Matrices for Direct Transcription

Orthogonal Collocation Matrices

$$N_{2 \times 2} = \begin{bmatrix} 0.75 & -0.25 \\ 1.00 & 0.00 \end{bmatrix} \quad (\text{A.5})$$

$$N_{3 \times 3} = \begin{bmatrix} 0.436 & -0.281 & 0.121 \\ 0.614 & 0.064 & 0.046 \\ 0.603 & 0.230 & 0.167 \end{bmatrix} \quad (\text{A.6})$$

$$N_{4 \times 4} = \begin{bmatrix} 0.278 & -0.202 & 0.169 & -0.071 \\ 0.398 & 0.069 & 0.064 & -0.031 \\ 0.387 & 0.234 & 0.278 & -0.071 \\ 0.389 & 0.222 & 0.389 & 0.000 \end{bmatrix} \quad (\text{A.7})$$

$$N_{5 \times 5} = \begin{bmatrix} 0.191 & -0.147 & 0.139 & -0.113 & 0.047 \\ 0.276 & 0.059 & 0.051 & -0.050 & 0.022 \\ 0.267 & 0.193 & 0.251 & -0.114 & 0.045 \\ 0.269 & 0.178 & 0.384 & 0.032 & 0.019 \\ 0.269 & 0.181 & 0.374 & 0.110 & 0.067 \end{bmatrix} \quad (\text{A.8})$$

Listing 3: MATLAB Dynamic Estimation

```

1 % Add path to APM MATLAB libraries
2 addpath('apm');
3 % Clear MATLAB
4 clear all; close all; clc
5 % Server and Application name
6 s = 'http://xps.apmonitor.com';
7 a = 'prbs';
8 % Clear previous application
9 apm(s,a,'clear all');
10 % Load model and data
11 apm_load(s,a,'4tank.apm');
12 csv_load(s,a,'prbs360.csv');
13 % Set up variable classifications
14 % Feedforwards
15 apm_info(s,a,'FV','km');
16 apm_info(s,a,'FV','kb');
17 apm_info(s,a,'FV','gamma[1]');
18 apm_info(s,a,'FV','gamma[2]');
19 apm_info(s,a,'FV','c13');
20 apm_info(s,a,'FV','c24');
21 % State variables
22 apm_info(s,a,'SV','h[3]');
23 apm_info(s,a,'SV','h[4]');
24 % Controlled variables
25 apm_info(s,a,'CV','h[1]');
26 apm_info(s,a,'CV','h[2]');
27 % Dynamic Estimation
28 apm_option(s,a,'nlc.imode',5);
29 % Read csv file
30 apm_option(s,a,'nlc.csv_read',1);
31 % Type (1=11-norm, 2=Squared Error)
32 apm_option(s,a,'nlc.ev_type',2);
33 % Time units (1=sec, 2=min, etc)
34 apm_option(s,a,'nlc.ctrl_units',1);
35 apm_option(s,a,'nlc.hist_units',2);
36 % Parameters to adjust
37 apm_option(s,a,'km.status',1);
38 apm_option(s,a,'km.lower',3);
39 apm_option(s,a,'km.upper',20);
40 apm_option(s,a,'kb.status',1);
41 apm_option(s,a,'kb.lower',-2);
42 apm_option(s,a,'kb.upper',2);
43 apm_option(s,a,'gamma[1].status',1);
44 apm_option(s,a,'gamma[1].lower',0.2);
45 apm_option(s,a,'gamma[1].upper',0.8);
46 apm_option(s,a,'gamma[2].status',1);
47 apm_option(s,a,'gamma[2].lower',0.2);
48 apm_option(s,a,'gamma[2].upper',0.8);
49 apm_option(s,a,'c13.status',1);
50 apm_option(s,a,'c13.lower',0.01);
51 apm_option(s,a,'c13.upper',0.2);
52 apm_option(s,a,'c24.status',1);
53 apm_option(s,a,'c24.lower',0.01);
54 apm_option(s,a,'c24.upper',0.2);
55 % Measured values
56 apm_option(s,a,'h[1].fstatus',1);
57 apm_option(s,a,'h[2].fstatus',1);
58 % Solver (1=APOPT, 3=IPOPT)
59 apm_option(s,a,'nlc.solver',3);
60 % Solve with APMonitor
61 apm(s,a,'solve');
62 % Open web-viewer
63 apm_web(s,a);
64 % Retrieve solution
65 solution = apm_sol(s,a);

```

Python Dynamic Estimation

```

# Import APM Package for Python
from apm import *

# Server and Application name
s = 'http://xps.apmonitor.com'
a = 'prbs'

# Clear previous application
apm(s,a,'clear all')

# Load model and data
apm_load(s,a,'4tank.apm')
csv_load(s,a,'prbs360.csv')

# Set up variable classifications
# Feedforwards
apm_info(s,a,'FV','km')
apm_info(s,a,'FV','kb')
apm_info(s,a,'FV','gamma[1]')
apm_info(s,a,'FV','gamma[2]')
apm_info(s,a,'FV','c13')
apm_info(s,a,'FV','c24')

# State variables
apm_info(s,a,'SV','h[3]')
apm_info(s,a,'SV','h[4]')

# Controlled variables
apm_info(s,a,'CV','h[1]')
apm_info(s,a,'CV','h[2]')

# Dynamic Estimation
apm_option(s,a,'nlc.imode',5)

# Read csv file
apm_option(s,a,'nlc.csv_read',1)

# Type (1=11-norm, 2=Squared Error)
apm_option(s,a,'nlc.ev_type',2)

# Time units (1=sec, 2=min, etc)
apm_option(s,a,'nlc.ctrl_units',1)
apm_option(s,a,'nlc.hist_units',2)

# Parameters to adjust
apm_option(s,a,'km.status',1)
apm_option(s,a,'km.lower',3)
apm_option(s,a,'km.upper',20)
apm_option(s,a,'kb.status',1)
apm_option(s,a,'kb.lower',-2)
apm_option(s,a,'kb.upper',2)
apm_option(s,a,'gamma[1].status',1)
apm_option(s,a,'gamma[1].lower',0.2)
apm_option(s,a,'gamma[1].upper',0.8)
apm_option(s,a,'gamma[2].status',1)
apm_option(s,a,'gamma[2].lower',0.2)
apm_option(s,a,'gamma[2].upper',0.8)
apm_option(s,a,'c13.status',1)
apm_option(s,a,'c13.lower',0.01)
apm_option(s,a,'c13.upper',0.2)
apm_option(s,a,'c24.status',1)
apm_option(s,a,'c24.lower',0.01)
apm_option(s,a,'c24.upper',0.2)

# Measured values
apm_option(s,a,'h[1].fstatus',1)
apm_option(s,a,'h[2].fstatus',1)

# Solver (1=APOPT, 3=IPOPT)
apm_option(s,a,'nlc.solver',3)

# Solve with APMonitor
apm(s,a,'solve')

# Open web-viewer
apm_web(s,a)

# Retrieve solution
(y,solution) = apm_sol(s,a)

```

557 **Appendix D. Nonlinear Control of the Quadruple Tank Process**

558 The MATLAB and Python scripts in Listing 4 detail the commands necessary
 559 to reproduce the nonlinear controller presented in this paper. The model file is
 560 the same as is shown in Appendix B but updated with new parameters from
 561 Table 4.

Listing 4: MATLAB Nonlinear Control

```

1 addpath('apm');
2 % Clear MATLAB
3 clear all; close all; clc
4 % Server and Application Name
5 s = 'http://xps.apmonitor.com';
6 a = 'nlc';
7 % Clear previous application
8 apm(s,a,'clear all');
9 % Load model
10 apm_load(s,a,'4tank_nlc.apm');
11 % Load future time horizon
12 csv_load(s,a,'control.csv');
13 % Set up variable classifications
14 % Feedforwards
15 apm_info(s,a,'FV','gamma[1]');
16 apm_info(s,a,'FV','gamma[2]');
17 % Manipulated variables
18 apm_info(s,a,'MV','v1');
19 apm_info(s,a,'MV','v2');
20 % State variables
21 apm_info(s,a,'SV','h[3]');
22 apm_info(s,a,'SV','h[4]');
23 % Controlled variables
24 apm_info(s,a,'CV','h[1]');
25 apm_info(s,a,'CV','h[2]');
26 % Steady state initialization
27 apm_option(s,a,'nlc.imode',3);
28 apm(s,a,'solve');
29 % Dynamic control
30 apm_option(s,a,'nlc.imode',6);
31 % Internal nodes
32 apm_option(s,a,'nlc.nodes',3);
33 % Time units (1=sec, 2=min, etc)
34 apm_option(s,a,'nlc.ctrl_units',1);
35 apm_option(s,a,'nlc.hist_units',2);
36 % Read csv file
37 apm_option(s,a,'nlc.csv_read',1);
38 % Manipulated variable tuning
39 apm_option(s,a,'v1.status',1);
40 apm_option(s,a,'v1.upper',6);
41 apm_option(s,a,'v1.lower',1);
42 apm_option(s,a,'v1.dmax',1);
43 apm_option(s,a,'v1.dcost',1);
44 apm_option(s,a,'v2.status',1);
45 apm_option(s,a,'v2.upper',6);
46 apm_option(s,a,'v2.lower',1);
47 apm_option(s,a,'v2.dmax',1);
48 apm_option(s,a,'v2.dcost',1);
49 % Controlled variable tuning
50 apm_option(s,a,'h[1].status',1);
51 apm_option(s,a,'h[1].fstatus',0);
52 apm_option(s,a,'h[1].sphi',10.1);
53 apm_option(s,a,'h[1].splo',9.9);
54 apm_option(s,a,'h[1].tau',10);
55 apm_option(s,a,'h[2].status',1);
56 apm_option(s,a,'h[2].fstatus',0);
57 apm_option(s,a,'h[2].sphi',15.1);
58 apm_option(s,a,'h[2].splo',14.9);
59 apm_option(s,a,'h[2].tau',10);
60 % Set controller mode
61 apm_option(s,a,'nlc.reqctrlmode',3);
62 % Run APMonitor
63 apm(s,a,'solve');
64 % Open web-viewer
65 apm_web(s,a);
66 % Retrieve solution
67 solution = apm_sol(s,a);
  
```

562

Python Nonlinear Control

```

from apm import *

# Server and Application Name
s = 'http://xps.apmonitor.com'
a = 'nlc'

# Clear previous application
apm(s,a,'clear all')

# load model
apm_load(s,a,'4tank_nlc.apm')

# load future time horizon
csv_load(s,a,'control.csv')

# Set up variable classifications
# Feedforwards
apm_info(s,a,'FV','gamma[1]')
apm_info(s,a,'FV','gamma[2]')

# Manipulated variables
apm_info(s,a,'MV','v1')
apm_info(s,a,'MV','v2')

# State variables
apm_info(s,a,'SV','h[3]')
apm_info(s,a,'SV','h[4]')

# Controlled variables
apm_info(s,a,'CV','h[1]')
apm_info(s,a,'CV','h[2]')

# Steady state initialization
apm_option(s,a,'nlc.imode',3)
apm(s,a,'solve')

# Dynamic control
apm_option(s,a,'nlc.imode',6)

# Internal nodes in the collocation
apm_option(s,a,'nlc.nodes',3)

# Time units (1=sec, 2=min, etc)
apm_option(s,a,'nlc.ctrl_units',1)
apm_option(s,a,'nlc.hist_units',2)

# Read csv file
apm_option(s,a,'nlc.csv_read',1)

# Manipulated variable tuning
apm_option(s,a,'v1.status',1)
apm_option(s,a,'v1.upper',6)
apm_option(s,a,'v1.lower',1)
apm_option(s,a,'v1.dmax',1)
apm_option(s,a,'v1.dcost',1)
apm_option(s,a,'v2.status',1)
apm_option(s,a,'v2.upper',6)
apm_option(s,a,'v2.lower',1)
apm_option(s,a,'v2.dmax',1)
apm_option(s,a,'v2.dcost',1)

# Controlled variable tuning
apm_option(s,a,'h[1].status',1)
apm_option(s,a,'h[1].fstatus',0)
apm_option(s,a,'h[1].sphi',10.1)
apm_option(s,a,'h[1].splo',9.9)
apm_option(s,a,'h[1].tau',10)
apm_option(s,a,'h[2].status',1)
apm_option(s,a,'h[2].fstatus',0)
apm_option(s,a,'h[2].sphi',15.1)
apm_option(s,a,'h[2].splo',14.9)
apm_option(s,a,'h[2].tau',10)

# Set controller mode
apm_option(s,a,'nlc.reqctrlmode',3)

# Run APMonitor
apm(s,a,'solve')

# Open web-viewer
apm_web(s,a)

# Retrieve solution
(y,solution) = apm_sol(s,a)
  
```

563 **References**

- 564 [1] M. L. Darby, M. Nikolaou, MPC: Current practice and challenges, *Control*
565 *Engineering Practice* 20 (4) (2012) 328–342.
- 566 [2] S. Qin, T. Badgwell, A survey of industrial model predictive control tech-
567 nology, *Control Engineering Practice* 11 (2003) 733–764.
- 568 [3] D. Gyalistras, S. Pr, C. Sagerschnig, M. Morari, Modeling and Identifica-
569 tion of a Large Multi-Zone Office Building, in: *IEEE International Confer-*
570 *ence on Control Applications (CCA)*, Vol. 17, 2011, pp. 55–60.
- 571 [4] F. Oldewurtel, A. Parisio, C. Jones, M. Morari, D. Gyalistras, M. Gwerder,
572 V. Stauch, B. Lehmann, K. Wirth, Energy efficient building climate con-
573 trol using stochastic model predictive control and weather predictions, in:
574 *American Control Conference (ACC)*, 2010, pp. 5100–5105.
- 575 [5] K. Nolde, M. Uhr, M. Morari, Medium term scheduling of a hydro-thermal
576 system using stochastic model predictive control, *Automatica* 44 (2008)
577 1585–1594.
- 578 [6] F. Oldewurtel, C. N. Jones, M. Morari, A tractable approximation of chance
579 constrained stochastic MPC based on affine disturbance feedback, 2008
580 47th *IEEE Conference on Decision and Control* (2008) 4731–4736.
- 581 [7] G. Papafotiou, T. Geyer, M. Morari, A hybrid model predictive control
582 approach to the direct torque control problem of induction motors, *Inter-*
583 *national Journal of Robust and Nonlinear Control* 17 (2007) 1572–1589.
- 584 [8] A. Bemporad, M. Morari, V. Dua, E. Pistokopoulos, The explicit linear
585 quadratic regulator for constrained systems, *Automatica* 38 (2002) 3–20.
- 586 [9] J. Hedengren, T. Edgar, Approximate nonlinear model predictive control
587 with in situ adaptive tabulation, *Computers and Chemical Engineering* 32
588 (2008) 706–714.
- 589 [10] T. Johansen, Approximate explicit receding horizon control of constrained
590 nonlinear systems, *Automatica* 40 (2004) 293–300.
- 591 [11] A. Domahidi, M. N. Zeilinger, M. Morari, C. N. Jones, Learning a feasible
592 and stabilizing explicit model predictive control law by robust optimiza-
593 tion, *IEEE Conference on Decision and Control and European Control*
594 *Conference* (2011) 513–519.
- 595 [12] H. J. Ferreau, H. G. Bock, M. Diehl, An online active set strategy to
596 overcome the limitations of explicit MPC, *International Journal of Robust*
597 *and Nonlinear Control* 18 (2008) 816–830.
- 598 [13] G. Pannocchia, J. B. Rawlings, S. J. Wright, Fast, large-scale model pre-
599 dictive control by partial enumeration, *Automatica* 43 (5) (2007) 852–860.

- 600 [14] R. Findeisen, F. Allgöwer, L. Biegler, Assessment and future directions of
601 nonlinear model predictive control, Springer-Verlag, Berlin, 2007.
- 602 [15] J. Hedengren, APMonitor Modeling Language, URL
603 <http://APMonitor.com> (2014).
- 604 [16] J. Hedengren, APMonitor modeling language for mixed-integer differential
605 algebraic systems, in: Computing Society Session on Optimization Mod-
606 eling Software: Design and Applications, INFORMS National Meeting,
607 Phoenix, AZ, 2012.
- 608 [17] M. Cizniar, D. Salhi, M. Fikar, M. Latifi, A MATLAB package for orthogo-
609 nal collocations on finite elements in dynamic optimisation, in: Proceedings
610 of the 15th Int. Conference Process Control '05, Strbske Pleso, Slovakia,
611 2005.
- 612 [18] B. Houska, H. J. Ferreau, M. Diehl, ACADO toolkit - An open-source
613 framework for automatic control and dynamic optimization, Optimal Con-
614 trol Applications and Methods 32 (2011) 298–312.
- 615 [19] P. Piela, A. Westerberg, K. Westerberg, T. Epperly, ASCEND: an object-
616 oriented computer environment for modeling and analysis: The modeling
617 language, Computers & Chemical Engineering 15 (1991) 53–72.
- 618 [20] H. Tummescheit, M. Gäfvert, T. Bergdahl, K.-E. Årzén, J. Åkesson, Mod-
619 eling and optimization with Optimica and JModelica.org Languages and
620 tools for solving large-scale dynamic optimization problems, Computers &
621 Chemical Engineering 34 (2010) 1737–1749.
- 622 [21] L. Simon, Z. Nagy, K. Hungerbuehler, Nonlinear Model Predictive Control,
623 Lecture Notes in Control and Information Sciences, Springer-Verlag Berlin
624 Heidelberg, 2009, Ch. Swelling Constrained Control of an Industrial Batch
625 Reactor Using a Dedicated NMPC Environment: OptCon, pp. 531–539.
- 626 [22] Z. Nagy, B. Mahn, R. Franke, F. Allgöwer, Evaluation study of an effi-
627 cient output feedback nonlinear model predictive control for temperature
628 tracking in an industrial batch reactor, Control Engineering Practice 15 (7)
629 (2007) 839–850.
- 630 [23] J. Hedengren, J. Mojica, W. Cole, T. Edgar, APOPT: MINLP solver for
631 differential and algebraic systems with benchmark testing, in: INFORMS
632 National Meeting, Phoenix, AZ, 2012.
- 633 [24] A. Wächter, L. Biegler, On the implementation of a primal-dual interior
634 point filter line search algorithm for large-scale nonlinear programming,
635 Mathematical Programming 106 (1) (2006) 25–57.
- 636 [25] C. S. Abbott, E. L. Haseltine, R. A. Martin, J. D. Hedengren, New capabil-
637 ities for large-scale models in computational biology, in: AIChE National
638 Meeting, Pittsburgh, PA, 2012.

- 639 [26] L. Sun, J. Hedengren, R. Beard, Optimal trajectory generation using model
640 predictive control for aerially towed cable systems, *Journal of Guidance,
641 Control, and Dynamics* 37 (2) (2014) 525–539.
- 642 [27] T. Soderstrom, Y. Zhang, J. Hedengren, Advanced process control in
643 Exxonmobil Chemical Company: Successes and challenges, in: *AICHE Na-
644 tional Meeting*, Salt Lake City, UT, 2010.
- 645 [28] L. Jacobsen, B. Spivey, J. Hedengren, Model predictive control with a
646 rigorous model of a solid oxide fuel cell, in: *Proceedings of the American
647 Control Conference (ACC)*, Washington, D.C., 2013, pp. 3747–3752.
- 648 [29] B. Spivey, J. Hedengren, T. Edgar, Constrained control and optimization
649 of tubular solid oxide fuel cells for extending cell lifetime, in: *Proceedings
650 of the American Control Conference (ACC)*, Montreal, Canada, 2012, pp.
651 1356–1361.
- 652 [30] B. Spivey, J. Hedengren, T. Edgar, Constrained nonlinear estimation for
653 industrial process fouling, *Industrial & Engineering Chemistry Research*
654 49 (17) (2010) 7824–7831.
- 655 [31] K. Jensen, J. Hedengren, Improved load following of a boiler with advanced
656 process control, in: *AICHE Spring Meeting*, Houston, TX, 2012.
- 657 [32] K. Powell, J. Hedengren, T. Edgar, Dynamic optimization of a solar ther-
658 mal energy storage system over a 24 hour period using weather forecasts,
659 in: *Proceedings of the American Control Conference (ACC)*, Washington,
660 D.C., 2013, pp. 2952–2957.
- 661 [33] K. M. Powell, T. F. Edgar, Control of a large scale solar thermal energy
662 storage system, *Proceedings of the 2011 American Control Conference* 2
663 (2011) 1530–1535.
- 664 [34] K. M. Powell, T. F. Edgar, Modeling and control of a solar thermal power
665 plant with thermal energy storage, *Chemical Engineering Science* 71 (2012)
666 138–145.
- 667 [35] J. Hedengren, D. Brower, Advanced process monitoring of flow assurance
668 with fiber optics, in: *AICHE Spring Meeting*, Houston, TX, 2012.
- 669 [36] D. Brower, J. Hedengren, C. Loegering, A. Brower, K. Witherow, K. Win-
670 ter, Fiber optic monitoring of subsea equipment, in: *Ocean, Offshore &
671 Arctic Engineering OMAE*, no. 84143, Rio de Janeiro, Brazil, 2012.
- 672 [37] D. Brower, J. Hedengren, R. A. Shishivan, A. Brower, Advanced deepwater
673 monitoring system, in: *Ocean, Offshore & Arctic Engineering OMAE*, no.
674 10920, Nantes, France, 2013.
- 675 [38] I. Nielsen, Modeling and control of friction stir welding in 5 cm thick copper
676 canisters, Master’s thesis, Linkping University (2012).

- 677 [39] H. Genceli, M. Nikolaou, Robust stability analysis of constrained ℓ_1 -norm
678 model predictive control, *AICHE Journal* 39 (1993) 1954–1965.
- 679 [40] C. E. Garcia, D. M. Prett, M. Morari, Model Predictive Control : Theory
680 and Practice a Survey, *Automatica* 25 (1989) 335–348.
- 681 [41] M. Nikolaou, Model predictive controllers: A critical synthesis of theory
682 and industrial needs, Vol. 26 of *Advances in Chemical Engineering*, Academic Press, 2001, pp. 131 – 204.
- 683
- 684 [42] L. T. Biegler, An overview of simultaneous strategies for dynamic optimization,
685 *Chemical Engineering and Processing: Process Intensification* 46 (11)
686 (2007) 1043 – 1053.
- 687 [43] J. Hedengren, Pendulum motion in the APMonitor Modeling Language,
688 URL <http://APMonitor.com/wiki/index.php/Apps/PendulumMotion>
689 (2014).
- 690 [44] T. J. Barth, D. E. Keyes, D. Roose, *Advances in Automatic Differentiation*,
691 Engineering 64.
- 692 [45] Z. Abul-el-zeet, P. Roberts, Enhancing model predictive control using dynamic
693 data reconciliation, *AICHE Journal* 48 (2) (2002) 324–333.
- 694 [46] M. Liebman, T. Edgar, L. Lasdon, Efficient data reconciliation and estimation
695 for dynamic processes using nonlinear programming techniques,
696 *Computers and Chemical Engineering* 16 (1992) 963–986.
- 697 [47] K. McBrayer, T. Edgar, Bias detection and estimation in dynamic data
698 reconciliation, *Journal of Process Control* 5 (4) (1995) 285–289.
- 699 [48] T. Soderstrom, T. Edgar, L. Russo, R. Young, Industrial application of a
700 large-scale dynamic data reconciliation strategy, *Industrial and Engineering
701 Chemistry Research* 39 (2000) 1683–1693.
- 702 [49] Y. Ramamurthi, P. Sistu, B. Bequette, Control-relevant dynamic data reconciliation
703 and parameter estimation, *Computers and Chemical Engineering* 17 (1) (1993) 41–59.
- 704
- 705 [50] J. S. Albuquerque, L. T. Biegler, Data reconciliation and gross-error detection
706 for dynamic systems, *AICHE Journal* 42 (1996) 2841–2856.
- 707 [51] N. Arora, L. T. Biegler, A Trust Region SQP Algorithm for Equality Constrained
708 Parameter Estimation with Simple Parameter Bounds, *Computational Optimization and Applications* 28 (2004) 51–86.
- 709
- 710 [52] L. T. Biegler, N. Arora, Redescending estimators for data reconciliation
711 and parameter estimation, *Computers & Chemical Engineering* 25 (2001)
712 1585–1599.

- 713 [53] E. P. Gatzke, F. J. Doyle III, Use of multiple models and qualitative knowl-
714 edge for on-line moving horizon disturbance estimation and fault diagnosis,
715 *Journal of Process Control* 12 (2) (2002) 339–352.
- 716 [54] R. Mahadevan, F. Doyle III, A partial flatness approach to nonlinear mov-
717 ing horizon estimation, *Proceedings of the 2004 American Control Confer-*
718 *ence* (2004) 211–215.
- 719 [55] A. Voelker, K. Kouramas, E. N. Pistikopoulos, Moving horizon estimation:
720 Error dynamics and bounding error sets for robust control, *Automatica* 49
721 (2013) 943–948.
- 722 [56] I. Landau, R. Lozano, M. M'Saad, A. Karimi, *Adaptive Control: Algo-*
723 *rithms, Analysis and Applications*, 2nd Edition, Communications and Con-
724 *trol Engineering*, Springer-Verlag, London, 2011.
- 725 [57] J. Ramlal, V. Naidoo, K. Allsford, J. Hedengren, Moving horizon estima-
726 tion for an industrial gas phase polymerization reactor, in: *Proc. IFAC*
727 *Symposium on Nonlinear Control Systems Design (NOLCOS)*, Pretoria,
728 South Africa, 2007.
- 729 [58] T. Binder, L. Blank, H. Bock, R. Burlisch, W. Dahmen, M. Diehl, T. Kro-
730 nseeder, W. Marquardt, J. Schlöder, O. Stryk, *Online Optimization of Large*
731 *Scale Systems*, Springer-Verlag Berlin Heidelberg, 2001, Ch. Introduction
732 to model based optimization of chemical processes on moving horizons, pp.
733 295–339.
- 734 [59] W. Shaohua, A. Kevin, T. Harris, K. McAuley, Selection of optimal param-
735 eter set using estimability analysis and MSE-based model-selection crite-
736 rion, *International Journal of Advanced Mechatronic Systems* 3 (3) (2011)
737 188–197.
- 738 [60] J. Hedengren, K. Allsford, J. Ramlal, Moving horizon estimation and con-
739 trol for an industrial gas phase polymerization reactor, in: *Proceedings of*
740 *the American Control Conference (ACC)*, New York, NY, 2007, pp. 1353–
741 1358.
- 742 [61] L. Biegler, S. Campbell, V. Mehrmann, *Control and Optimization with*
743 *Differential-Algebraic Constraints*, SIAM - Society for Industrial and Ap-
744 *plied Mathematics*, Philadelphia, 2012.
- 745 [62] J. Albuquerque, L. Biegler, Decomposition algorithms for on-line estima-
746 tion with nonlinear DAE models, *Computers and Chemical Engineering*
747 21 (3) (1997) 283–299.
- 748 [63] M. Diehl, H. G. Bock, J. P. Schlöder, R. Findeisen, Z. Nagy, , F. Allgöwer,
749 Real-time optimization and nonlinear model predictive control of processes
750 governed by differential-algebraic equations, *Journal of Process Control* 12
751 (2002) 577–585.

- 752 [64] E. Haseltine, J. Rawlings, Critical evaluation of extended kalman filtering
753 and moving-horizon estimation, *Ind. Eng. Chem. Res.* 44 (8) (2005) 2451–
754 2460.
- 755 [65] B. Odelson, M. Rajamani, J. Rawlings, A new autocovariance least-squares
756 method for estimating noise covariances, *Automatica* 42 (2) (2006) 303–308.
- 757 [66] J. Hedengren, T. Edgar, Moving horizon estimation - the explicit solution,
758 in: *Proceedings of Chemical Process Control (CPC) VII Conference*, Lake
759 Louise, Alberta, Canada, 2006.
- 760 [67] B. Spivey, J. Hedengren, T. Edgar, Monitoring of process fouling using
761 first-principles modeling and moving horizon estimation, in: *Proc. Texas*,
762 Wisconsin, California Control Consortium (TWCCC), Austin, TX, 2009.
- 763 [68] M. Darby, M. Nikolaou, J. Jones, D. Nicholson, RTO: An overview and
764 assessment of current practice, *Journal of Process Control* 21 (2011) 874–
765 884.
- 766 [69] G. Carey, B. Finlayson, Othogonal collocation on finite elements, *Chemical*
767 *Engineering Science* 30 (1975) 587–596.
- 768 [70] J. S. Albuquerque, L. T. Biegler, Decomposition algorithms for on-line
769 estimation with nonlinear models, *Computers & Chemical Engineering* 19
770 (1995) 1031–1039.
- 771 [71] K. Johansson, Interaction bounds in multivariable control systems, *Auto-*
772 *matica* 38 (6) (2002) 1045–1051.
- 773 [72] T. Raff, S. Huber, Z. K. Nagy, F. Allgöwer, Nonlinear model predictive con-
774 trol of a four tank system: An experimental stability study, in: *Proceedings*
775 *of International Conference Control Applications*, Munich, Germany, 2006,
776 pp. 237–242.
- 777 [73] E. Gatzke, E. Meadows, C. Wang, F. Doyle III, Model based control of a
778 four-tank system, *Computers and Chemical Engineering* 24 (2000) 1503–
779 1509.
- 780 [74] K. Johansson, The quadruple-tank process - a multivariable laboratory
781 process with an adjustable zero, *IEEE Transactions on Control Systems*
782 *Technology* 8 (3) (2000) 456–465.
- 783 [75] I. Drca, Nonlinear model predictive control of the four tank process, Mas-
784 ter’s thesis, Universidad de Sevilla (2007).
- 785 [76] M. Mercangöz, F. Doyle III, Distributed model predictive control of an
786 experimental four-tank system, *Journal of Process Control* 17 (3) (2007)
787 297–308.

- 788 [77] I. Alvarado, D. Limon, D. M. noz de la Peña, J. Maestre, M. Ridaio,
789 H. Scheu, W. Marquardt, R. Negenborn, B. D. Schutter, F. Valencia,
790 J. Espinosa, A comparative analysis of distributed MPC techniques ap-
791 plied to the HD-MPC four-tank benchmark, *Journal of Process Control*
792 21 (5) (2011) 800–815.
- 793 [78] L. Biegler, *Nonlinear Programming: Concepts, Algorithms, and Applica-*
794 *tions to Chemical Processes*, Society for Industrial and Applied Mathemat-
795 ics and the Mathematical Optimization Society, 2010.
- 796 [79] C. Rao, J. Rawlings, Linear programming and model predictive control,
797 *Journal of Process Control* 10 (2000) 283–289.
- 798 [80] P. Dave, D. Willig, G. Kudva, J. Pekny, F. Doyle III, LP methods in MPC
799 of large-scale systems: Application to paper-machine CD control, *AIChE*
800 *Journal* 43 (1997) 1016–1031.
- 801 [81] P. Dave, F. Doyle III, J. Pekny, Customization strategies for the solution
802 of linear programming problems arising from large scale model predictive
803 control of a paper machine, *Journal of Process Control* 9 (1999) 385–396.
- 804 [82] J. Hedengren, MATLAB toolbox for the APMonitor Modeling Language,
805 URL <http://APMonitor.com/wiki/index.php/Main/MATLAB> (2014).
- 806 [83] J. Hedengren, Python toolbox for the APMonitor Modeling Language, URL
807 <http://APMonitor.com/wiki/index.php/Main/PythonApp> (2014).